Geophysical Research Letters

RESEARCH LETTER
10.1029/2019GL084444

Closure of Secondary Basins Causes Channel Deepening in Estuaries With Moderate to High Friction

A. Nnafie[1,2], H. E. de Swart[2], B. De Maerschalck[1], T. Van Oyen[1], M. van der Vegt[2], and M. van der Wegen[3,4]

[1]Flanders Hydraulics Research, Antwerp, Belgium, [2]IMAU, Utrecht University, Utrecht, The Netherlands, [3]IHE, Delft, The Netherlands, [4]Deltares, Delft, The Netherlands

Key Points:
- Connected secondary basins in estuaries with moderate to high friction cause the main channel to be shallower than those without such basins
- This shallowing is more pronounced for basins that are located at the northern estuarine margin due to the Coriolis force
- Closure of secondary basins decreases the tidal asymmetry driven sediment transport (landward-directed), resulting in channel deepening

Supporting Information:
- Supporting Information S1

Correspondence to:
A. Nnafie,
a.nnafie@uu.nl

Citation:
Nnafie, A., de Swart, H. E., De Maerschalck, B., Van Oyen, T., van der Vegt, M., & van der Wegen, M. (2019). Closure of secondary basins causes channel deepening in estuaries with moderate to high friction. *Geophysical Research Letters*, *46*, 13,209–13,216. https://doi.org/10.1029/2019GL084444

Received 21 JUL 2019
Accepted 26 OCT 2019
Accepted article online 19 NOV 2019
Published online 21 NOV 2019

Abstract Estuaries are often characterized by the presence of secondary basins (side embayments), which affect the estuarine hydrodynamics and sediment dynamics. Many of these basins have disappeared due to land reclamations, which might influence the estuarine morphodynamics. This study addresses how the presence and closure of secondary basins affect the estuarine channel depth using the Delft3D model. Results reveal that channels in estuaries with secondary basins are shallower than those in which these basins are absent, regardless of their location, length, or number. This shallowing is more pronounced for basins that are located at the northern estuarine margin due to the Coriolis force. The shallowing of channels increases if more secondary basins are present. Channels deepen after the closure of secondary basins, resulting from a decrease of the landward directed sediment transport that is driven by tidal asymmetry. Model results apply to estuaries with moderate to high friction.

1. Introduction

Estuarine margins are often characterized by the presence of side embayments (secondary basins [SBs]), whose areas are 1–20% of the total estuarine surface area (Nnafie et al., 2018). Land reclamations in the last centuries (Pye & Blott, 2014) have led to the disappearance of SB area in many estuaries (e.g., the Columbia River Estuary, Ems Estuary, Weser Estuary, and Western Scheldt Estuary) (Ahlhorn et al., 2012; Healy & Hickey, 2002; Sherwood et al., 1990; Van der Spek, 1997; Van Maren et al., 2016). SBs affect the hydrodynamics and sediment dynamics in estuaries (Alebregtse & de Swart, 2014; Li et al., 2016), suggesting that their disappearance may influence the estuarine morphodynamics. Compared to the main estuary, SBs are lower-energy areas (Yellen et al., 2017), which provide natural-sheltered harbors and serve as important sinks for fine sediments and nutrients (Woodruff et al., 2013). Therefore, SBs offer an ideal setting for the formation of mudflats and salt marshes, while vegetation on these marshes further enhances the trapping of nutrients and speeds up the siltation of fine sediments and organic material. Thus, reclaiming SB area could result in the degradation of estuarine ecosystems.

Historical bathymetric data reveal that channels in the Western Scheldt Estuary (Netherlands; Figure 1a) have deepened between 1800 and 2015, possibly resulting from the closure of its SBs (further details are given in section S1 of the supporting information). In the Weser Estuary (Germany), the closure of SBs and anabranches between 1883 and 1895 led to the subsequent deepening of the estuary (Ahlhorn et al., 2012; Lucker et al., 1995). The depth of intermediate channels (5–20 m) in the Columbia River Estuary (USA) increased between 1868 and 1958, possibly resulting from the reduction of its SB area during this time span (Sherwood et al., 1990). Channel deepening often leads to a higher tidal range, which might increase suspended sediment concentrations and reduce nutrients in estuaries (Winterwerp et al., 2013).

This study aims to investigate to what extent the disappearance of SBs has contributed to the observed deepening in estuaries, given the fact that the latter also experienced major engineering works (e.g., the construction of jetties and channel dredging) that might have also caused this deepening. The specific objectives are fourfold. The first is to investigate the effects of the presence of SBs on the long-term evolution (order decades to centuries) of the estuarine channel depth. The second is to examine how the depth of channels, which have formed in the presence of SBs, changes after the closure of these basins. The third objective is to unravel the physical mechanisms that cause differences in channel depth when SBs are present or absent and, finally, to explore how these differences depend on the characteristics of the tidal forcing at the seaward boundary, estuary depth, and estuary length. To address these objectives, the model Delft3D is used.

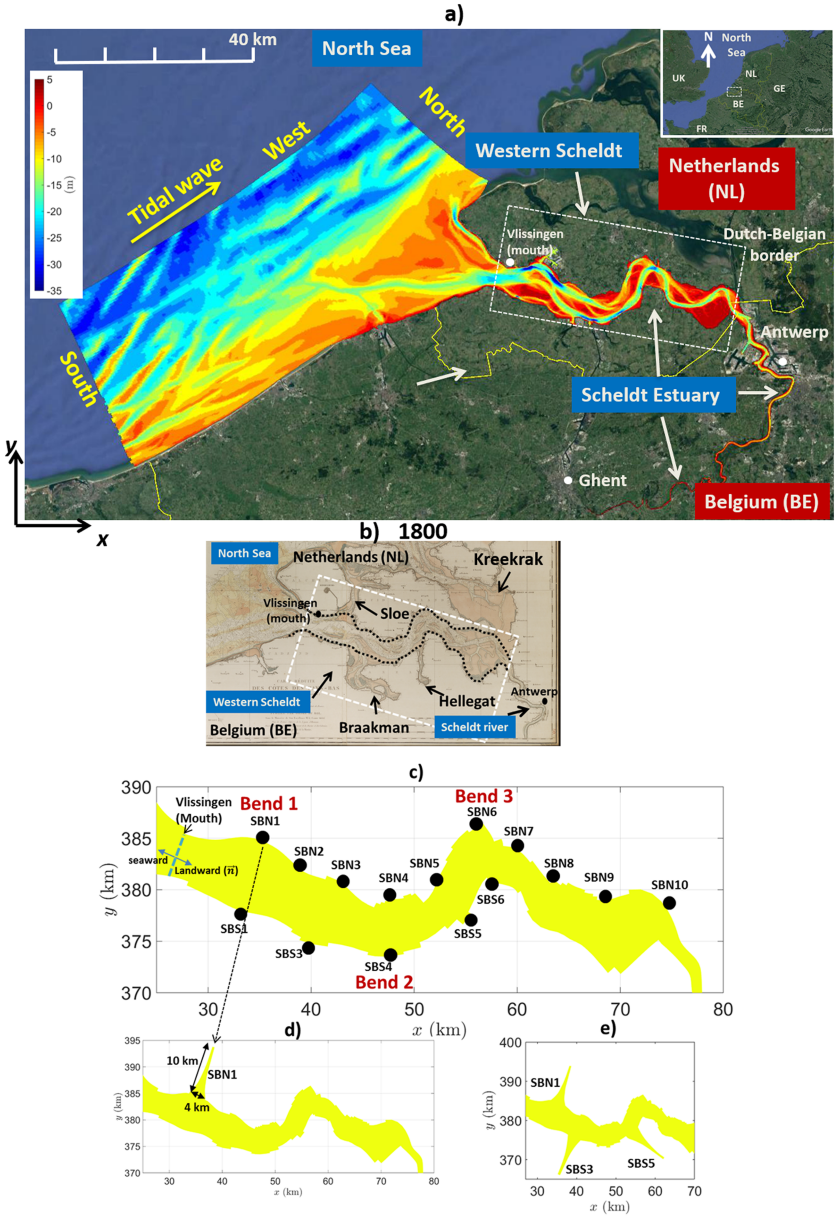

Figure 1. (a) The present-day bed level z_b of the Western Scheldt (WS) (see the inset on top right for its location). (b) The geometric shape of WS in 1800 (source: Department Maritime Access, The Government of Flanders). Arrows indicate former secondary basins Sloe, Braakman, Hellegat, and Kreekrak. Black dotted lines denote the present-day geometric shape of the estuary. (c) Locations of secondary basins considered in this study (black dots). Colors indicate the initial bed level z_b used to start the simulations (approximately −10 m). (d,e) Geometric shapes of the estuary in the cases of one secondary basin (d) and three basins (e).

2. Methodology

2.1. Study Area

This study considers an estuary with a geometric shape that is based on the present-day Western Scheldt Estuary (Figure 1a). This estuary (hereafter referred to as WS) is the marine part of the Scheldt Estuary (with length ~ 160 km); it extends over a distance L of about 60 km from Vlissingen (mouth) to the Dutch-Belgian border, and it has a mean depth H_0 (averaged over the total estuarine surface area) of about 10 m. Further details are given in section S1.

2.2. Model Description

The Delft3D model (depth-averaged mode) solves the mass and momentum balance, sediment transport, and bed level change on a curvilinear grid that covers the Scheldt Estuary and part of the North Sea

Table 1
List of Model Runs

Name runs	Description	SM
Reference	• Configuration of WS (no SB), $[\hat{\eta}_2, \hat{\eta}_4, \hat{\eta}_6] = [1.6, 0.1, 0.05]$ m, $[\phi_2, \phi_4, \phi_6] = [23, -11, -24]°$, $H_0 = 10$ m, $L \sim 60$ km.	500 years
SBN1	• 1 SB; located at $d = 1/10L \sim 6$ km from the mouth.	500 years
Single	• 1 SB: north (SBNi, $i = 2, 3, .., 9, 10$), south (SBSi, $i = 1, 3, 4, 5, 6$).	300 years
Double	• 2 SB: SBN1 + SBNi, $i = 2, 4, 6$; SBN1 + SBSi, $i = 1, 4, 5, 6$.	300 years
Triple	• 3 SB: SBN1 + SBS3 + SBS5.	1,000 years
Geometry	• SBN1-Short, SBN1-Long.	300 years
SBN1-SBS3-SBS5 ON/OFF	• $t \leq 300$ years: SBN1 + SBS3 + SBS5; • $t > 300$ years: all secondary basins are removed.	1,000 years
Hydro1	• Default setting, with/without SB, $t = [0 - 300]$ years.	10 tc
Hydro2	• With/without SB, $t = 0$ year, $\hat{\eta}_4/\hat{\eta}_2 = [0; 0.125]$, $\phi_4 - 2\phi_2 = [-180; 180]°$, $H_0 = [5; 20]$ m, length = [40; 160] km.	10 tc

Note. SBNi and SBSi mean that an SB is located at the northern and southern banks of the estuary, respectively, at distance $d = i/10L$ from the mouth. Here, i is an integer, and L is the length of WS. The third column shows the total simulation time (SM), either in years or in tidal cycles (tc).

(Figure 1a). Waves, wind, and sea-level rise are not considered. Noncohesive sand is assumed with a single size of $d_{50} = 200\mu$m. The model is forced by a water level η at the western boundary and a water level gradient normal to the southern and northern boundaries. This water level consists of harmonic constituents M_2, M_4, and M_6, having, respectively, amplitudes $\hat{\eta}_2$, $\hat{\eta}_4$, and $\hat{\eta}_6$ and phases ϕ_2, ϕ_4, and ϕ_6 (Table 1). Furthermore, zero gradients in the sediment concentration are imposed normal to the seaward boundaries, which minimize accretion or erosion near these boundaries (Deltares, 2016). At the landward boundary, near Ghent, the along-channel velocity and sediment transport vanish.

2.3. Experimental Design

2.3.1. Morphodynamic Runs

All morphodynamic experiments start from an initially flat bed ($z_b = -H_0 = -10$ m) until stable morphological patterns are obtained, which take 200 to 300 years (Nnafie et al., 2018). Results are compared with those of a reference case in which SBs are absent ("Reference" in Table 1). The default simulation time is 300 years. To make sure that results do not depend on this time, some experiments are run for longer periods. An overview of all experiments and their corresponding simulation times is given in Table 1.

The first experiment with an SB is "SBN1" (Table 1), where a single SB with length $l_b \sim 10$ km is placed at distance $d = 1/10L$ from the mouth (Figures 1c and 1d). The SB, which is placed perpendicular to the estuary axis, has a width w_b that decreases exponentially from 4 km at its transition to the estuary to ~ 0.5 km at its landward end.

Next, runs are conducted by placing the SB at either the northern (SBNi) or southern (SBSi) margins of the estuary at distance $d = i/10L$ (black dots in Figure 1c), where i is an integer (Table 1). Additional runs are performed with two and three basins (runs "Double" and "Triple"). In "Double," either two northern basins (SBN1 and SBNi, $i = 2, 4, 6$) or one northern basin (SBN1) and one southern basin (SBSi, $i = 1, 4, 5, 6$) are considered. In "Triple," the basins have approximately the same locations as those of former SBs of WS (Sloe, Braakman, and Hellegat; Figures 1b and 1e). Furthermore, two experiments are carried out ("Geometry"), where the length of SBN1 is, respectively, halved ($l_b = 5$km) and doubled ($l_b = 20$km) ("SBN1-Short" and "SBN1-Long").

Finally, an experiment is carried out ("SBN1-SBS3-SBS5 ON/OFF") with a simulation time of 1,000 years in the presence of three SBs (Figure 1e) between $t = 0$ and $t = 300$ years, after which these basins are removed for $t > 300$ years. The geometric shape of the estuary for $t \leq 300$ years mimics that of WS in 1800 (Figure 1b). The results are compared with those from "Triple," where the three SBs remain present during the entire simulation period.

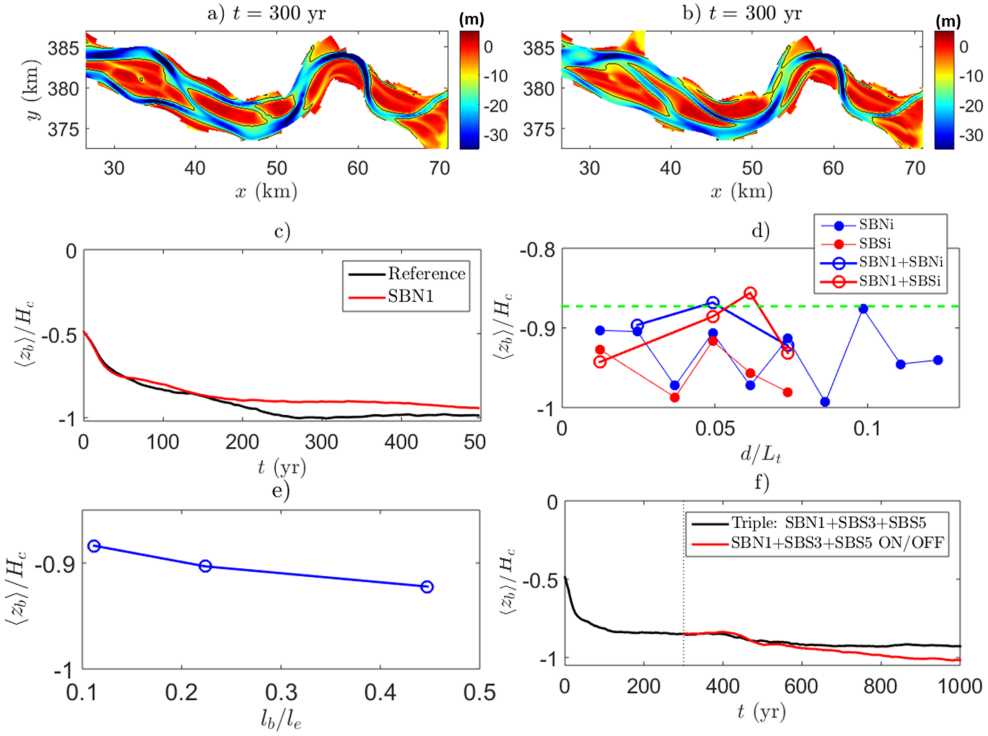

Figure 2. (a,b) The modeled bed level z_b in the cases "Reference" (a) and "SBN1" (b). (c) Dimensionless mean channel bed level $\langle z_b \rangle / H_c$ of the two cases versus time, where $H_c = -\langle z_b \rangle_{Ref} = 21.9$ m is the mean channel depth of the reference case (t = 300 years). (d) $\langle z_b \rangle / H_c$ at t = 300 years versus dimensionless distance d/L_t in the cases of either one single basin (SBNi and SBSi) or two basins (SBN1 + SBNi and SBN1 + SBSi). Length L_t is the frictionless tidal wavelength (≃450 km). In the case of two SBs, d is the distance of the second basin. For comparison, $\langle z_b \rangle$ of "Triple" is also shown (green line). (e) $\langle z_b \rangle / H_c$ at t = 300 years versus the length of the SB (l_b). Here, l_b is scaled with the tidal excursion length $l_e = 2\pi U/\omega \simeq 45$ km, with U the mean (basin-averaged) flow velocity in WS (~1 m/s) and ω is the M_2 frequency. (f) Time evolution of $\langle z_b \rangle / H_c$ in the cases "Triple" and "SBN1+SBS3+SBS5 ON/OFF."

The analysis of results focuses on the comparison between the mean bed level of channels ($\langle z_b \rangle$) of cases with and without SBs. Here, brackets $\langle \cdot \rangle$ denote an average over the total channel surface area for which $z_b < -H_0$. Other threshold values are also considered. Only channels that form in the main estuary (without SBs) are included in this comparison.

2.3.2. Hydrodynamic Runs

Two series of hydrodynamic simulations ("Hydro1" and "Hydro2") are conducted to identify the physical mechanisms that cause differences in $\langle z_b \rangle$ when SBs are present or absent and to explore how these differences depend on (1) the characteristics of the tidal forcing at the seaward boundary, (2) initial estuary depth H_0, and (3) estuary length. The characteristics of the tidal forcing are expressed by the ratio $\hat{\eta}_4/\hat{\eta}_2$ and by the phase difference $\phi_4 - 2\phi_2$. In "Hydro1," bathymetries of cases with and without an SB (SBN1) obtained from the morphodynamic runs at t = 0, 10, 50, 100, 150, 200, 300 years are used (flow over topography). In "Hydro2," the impact of the SB on the residual (i.e., tidally averaged) sediment transport is quantified for different values of $\hat{\eta}_4/\hat{\eta}_2$ (range [0; 0.125]) and $\phi_4 - 2\phi_2$ ([−180; 180]°), different values of depths H_0 ([5; 20] m) and of lengths ([40; 160] km).

Results from these simulations, which last 10 tidal cycles, are used to compute the residual transport $\overline{\vec{q} \cdot \vec{n}}$ through the mouth cross section (dashed blue line in Figure 1c). Here, $\vec{q}$ is the transport vector (in $m^3 \cdot s^{-1} \cdot m^{-1}$), $\vec{n}$ is a unit vector normal to the cross section (directed landward; Figure 1c), and the overbar (——) denotes an average over the last five tidal cycles. The first five cycles are excluded to avoid errors due to flow adjustment. Subsequently, the obtained result is integrated over the mouth section ($\langle \overline{\vec{q} \cdot \vec{n}} \rangle$; where brackets "$\langle \cdot \rangle$" indicate the integration). Positive (negative) values of $\langle \overline{\vec{q} \cdot \vec{n}} \rangle$ represent landward directed (seaward directed) transport. Finally, $\langle \overline{\vec{q} \cdot \vec{n}} \rangle$ is decomposed into contributions associated with the residual flow ($\langle \overline{\vec{T}_1 \cdot \vec{n}} \rangle$) and tidal asymmetry ($\langle \overline{\vec{T}_2 \cdot \vec{n}} \rangle$). Expressions for $\vec{T}_1$ and $\vec{T}_2$, as well as a list of all the abbreviations and symbols used in this manuscript, are given in Supporting Information S1.

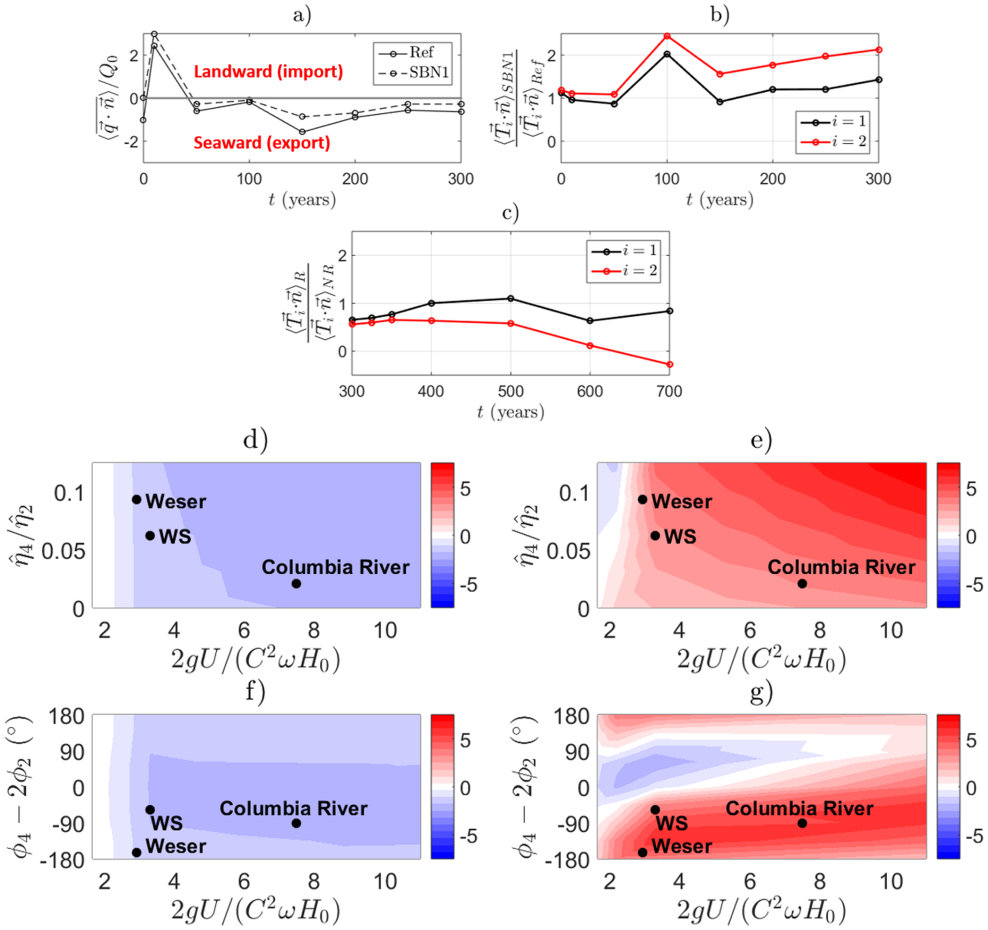

Figure 3. (a) Total residual sediment transport $\langle \overline{\vec{q} \cdot \vec{n}} \rangle$ through the mouth cross section versus time for cases "Reference" and "SBN1." Positive (negative) values indicate landward (seaward) transport. Transport $\langle \overline{\vec{q} \cdot \vec{n}} \rangle$ is scaled with its absolute value at $t = 0$ of the reference case ($Q_0 = |\langle \overline{\vec{q} \cdot \vec{n}} \rangle|_{\mathrm{Ref},t=0} = 0.05\ \mathrm{m^3 s^{-1}}$). (b) The ratio between components of the residual sediment transport related with residual flow ($\langle \vec{T}_1 \cdot \vec{n} \rangle$) and ratio between components related with tidal asymmetry ($\langle \vec{T}_2 \cdot \vec{n} \rangle$) of cases "Reference" and "SBN1." (c) As in (b) but showing ratios of cases with (R) and without (NR) removing the three SBs versus time. (d,e) Differences in transports $\langle \vec{T}_1 \cdot \vec{n} \rangle$ (d) and $\langle \vec{T}_2 \cdot \vec{n} \rangle$ (e) between cases "SBN1" and "Reference" at $t = 0$ for different ratios $\hat{\eta}_4/\hat{\eta}_2$ and dimensionless friction parameters $F = 2gU/(C^2\omega H_0)$. Here, C is the Chézy coefficient ($= 65\mathrm{m}^{1/2}\ \mathrm{s}^{-1}$), U is the mean flow velocity, and H_0 is the mean depth of the estuary. Values (U;H_0) for the different estuaries (indicated by the black filled circles) found in literature are WS → (1 ms^{-1}; 10 m); Weser Estuary: → (1.15 ms^{-1}; 13 m); and Columbia River Estuary: → (1.2 ms^{-1}; 5.3 m). (f,g) As in (d) and (e) but for different phase differences $\phi_4 - 2\phi_2$. Amplitudes and phases of the M_2 and M_4 components for the Weser and Columbia River estuaries were obtained from the TPXO global tidal data set (Egbert & Erofeeva, 2002).

3. Results

3.1. Presence of SBs

Figure 2 shows the modeled bed level in cases without (a) and with SBN1 (b) after evolving toward a state of low morphodynamic activity (i.e., bed level changes are less than 1% of the initial changes). Channels that form in the estuary in the case with an SB are shallower than those that form in the case without the basin (c), particularly those that form near SBN1 (Figure S4). Imposing other threshold values for the channel bed level ($z_b < -15$ m, $z_b < -7.5$ m, or $z_b < -5$ m) does not qualitatively change the results (Figure S5).

Channels that form in cases of other locations of the SB are also shallower than those of the reference case (Figure 2d). Overall, channel shallowing is less when the SB is located south compared to the one that is situated north. Additional runs (Figure S6) demonstrated that this difference is due to the Coriolis force. Figure 2d further shows that channels tend to become about 0.7 m shallower per added SB.

Finally, the results (Figure 2e) reveal that also for different lengths of the SB, channels are shallower compared with those of the reference case. This shallowing reduces for large lengths of the SB.

3.2. Closure of SBs

Figure 2f reveals that channels deepen over time (particularly in the central and seaward parts of the estuary; Figure S7) after the closure of basins SBN1, SBS3, and SBS5 ("SBN1+SBS3+SBS5 ON/OFF"), relative to the case in which these basins remain open during the entire simulation period ("Triple"). This deepening occurs about 150 years after removing the basins. Figure 2f further shows that channels continue to deepen after $t = 1,000$ years, thereby becoming deeper than the channels of the reference case.

3.3. Physical Mechanisms

The results (Figure 3a) reveal that in cases with and without an SB, the estuary initially ($t \leq 50$ years) imports sand (channel shallowing), while it exports sand for $t > 50$ years (channel deepening). However, in comparison to the reference case, the presence of an SB leads to a larger import of sediment into the estuary in the first 50 years (channels become more shallow), and it reduces the export from the estuary in the subsequent time period (less channel deepening). Hence, shallower channels form when adding an SB. Note that sediment exchanges between the estuary and other adjacent areas (SB area and area landward of the estuary) are not considered, as these exchanges are much smaller than those at the mouth.

It turns out that the differences between the sediment exchange at the mouth of the cases with and without an SB are mostly due to a larger tidal asymmetry-driven sediment transport $\langle \vec{T}_2 \cdot \vec{n} \rangle$ (Figure 3b), which is directed landward. On average, residual transport $\langle \vec{T}_1 \cdot \vec{n} \rangle$ (seaward directed) of the case with an SB is larger than that of the case without an SB, but this increase is not sufficient to compensate for the increase of landward directed transport $\langle \vec{T}_2 \cdot \vec{n} \rangle$ when adding an SB. As is detailed in Supporting Information S1, the increase of transports $\langle \vec{T}_1 \cdot \vec{n} \rangle$ and $\langle \vec{T}_2 \cdot \vec{n} \rangle$ through the mouth section when adding an SB is caused mainly by an increase of the M_2 velocity and a decrease of both the residual and the M_4 velocities. However, the decrease of the residual flow is stronger than that of the M_4 velocity. So, the landward directed sediment transport $\langle \vec{T}_2 \cdot \vec{n} \rangle$ through the mouth section increases more than the seaward directed sediment transport $\langle \vec{T}_1 \cdot \vec{n} \rangle$. Consequently, the estuary gains more sediment when adding an SB.

The closure of SBs decreases landward directed transport $\langle \vec{T}_2 \cdot \vec{n} \rangle$ (Figure 3c) but now resulting mainly from a reduction of the M_2 velocity. This reduction is due to a decline in the estuarine area resulting from this closure (Figure S8). In contrast, seaward directed transport $\langle \vec{T}_1 \cdot \vec{n} \rangle$ is less affected by the closure of SBs, because of a strong increase of the residual velocity that counteracts the decrease of the M_2 velocity. On the long term, the ratio between transports $\langle \vec{T}_2 \cdot \vec{n} \rangle$ of cases with and without closure of SBs even becomes negative, meaning that the transport of the former case is seaward directed. This is caused by changes in the phases of M_2 and M_4 velocities, such that the cosine of their relative phase becomes negative (seaward directed). Consequently, seaward directed transport $\langle \vec{T}_1 \cdot \vec{n} \rangle$ is now reinforced by transport $\langle \vec{T}_2 \cdot \vec{n} \rangle$, leading to enhanced sand export. An analysis of the total volumes of channels and shoals in cases with and without closure of SBs (Figure S9) reveals that the larger sand export in the former case is provided mainly by sand that is eroded from the channels (deepening).

3.4. Different Estuarine Configurations

Figures 3e and 3g show that the differences between $\langle \vec{T}_2 \cdot \vec{n} \rangle$ of cases with and without an SB are positive in most parts of the parameter spaces $(\hat{\eta}_4/\hat{\eta}_2, F)$ and $(\phi_4 - 2\phi_2, F)$. Here, $F = 2gU/(C^2\omega H_0)$ is the dimensionless friction number (Savenije et al., 2008), with C the Chézy coefficient, U the mean (domain-averaged) flow velocity, and H_0 the mean estuarine depth. Clearly, the presence of an SB leads to enhanced landward directed sediment transport due to tidal asymmetry. The presence of an SB increases the magnitude of the seaward directed residual transport (blue areas in d and f), but this increase is weaker than the increase in $\langle \vec{T}_2 \cdot \vec{n} \rangle$. Thus, the estuary tends to accumulate more sand when adding an SB, particularly in frictionally dominated estuaries (large F) that are subject to large ratios $\hat{\eta}_4/\hat{\eta}_2$ and large absolute values of $\phi_4 - 2\phi_2$. In contrast, estuaries with SBs and which are characterized by a weak friction (small F) and values of $\phi_4 - 2\phi_2$ roughly between 0° and 90° (blue area in Figure 3g) are expected to be deeper compared with those without the basins. This implies that the closure of SBs in this type of estuaries would cause channel shallowing. The tendency to accumulate more sand when adding an SB also occurs for different lengths of the estuary (Figure S10), although it seems that the presence of an SB in an estuary with a length close to the quarter tidal wavelength ($0.25L_t$) and with large ratios $\hat{\eta}_4/\hat{\eta}_2$ would trigger channel deepening.

4. Comparison With Observations

Additional experiments (section S3) show that the presence of SBs reduces not only the depth of channels but also their volume, suggesting that the disappearance of SBs in WS has contributed to the observed deepening

and volume increase of its channels (section S1). Figure S11 demonstrates that the reduction of the depth and volume of channels when adding SBs cannot be explained with the existing empirical relationship between the channel volume and tidal prism (Van der Wegen & Roelvink, 2008). This reduction is attributed to an increase in the tidal asymmetry-driven sediment transport (section 3.3).

A discrepancy between model outcomes and observations is that, after the closure of the basins, channels start to deepen after an adjustment time period (τ) of ~150 years, whereas the observed deepening in WS seems to take place more rapidly (order tens of years; section S1). Figure S9 shows that, prior to channel deepening, shoals are losing sand during the adjustment period. This sand is mostly exported to the outer sea, suggesting that the excess of shoal volume (with respect to the reference case) at the time of closure ($V_s \sim 2.8 \times 10^8$ m^3) and the rate of sand export from the estuary ($Q \sim 0.05$ m^3/s) determine the time scale τ. Thus, $\tau \sim V_s/Q \sim 178$ years, which is a good estimate of the simulated time scale. A reason for this discrepancy might be the fact that channels of WS have been substantially dredged (Jeuken, 2000). Another reason is that sea-level rise might have also contributed to the deepening of WS, although Van der Wegen (2013) found that sea-level rise does not deepen channels over time. A third reason is that the tidal range in the North Sea increased during the last two centuries (Kuijper & Lescinski, 2012), which likely led to stronger tidal currents and enhanced channel erosion in WS.

Finally, the observed deepening of channels in the Weser and Columbia river estuaries (section 1) can be at least partly explained by the removal of their SB area. As is shown in Figures 3e and 3g (black dots), this removal caused a weakening of the landward directed tidal asymmetry-driven sediment transport.

5. Conclusions

Model results show that the mean depth of estuarine channels is smaller in the presence of SBs compared with that in the absence of these basins, particularly when these basins are located at the northern estuarine margin. This difference in depth occurs regardless of the location, length, or numbers of SBs. The larger the number of basins, the smaller the channel depth. Channels deepen over time after the closure of SBs. This agrees with observed depth changes in estuaries, such as the Western Scheldt, albeit that the simulated channel deepening takes place on a longer time scale compared with observations.

Model results demonstrate that the presence of SBs reduces the tendency of the estuary to export sediment, leading to channel shallowing. This is due to an increase of the tidal asymmetry-driven sediment transport (landward directed) through the mouth, resulting mainly from an increase in the M_2 velocity. In the case of closure of SBs, the tidal asymmetry-driven sediment transport decreases significantly, and it even becomes seaward directed, reinforcing the seaward directed sediment transport related with the residual flow. Finally, a sensitivity analysis suggests that the shallowing of channels due to the presence of SBs occurs in estuaries with moderate to high friction, where the tidal forcing has a large ratio between the amplitudes of the M_4 and M_2 water level components and a large absolute value of the phase difference between these components.

Acknowledgments
Rijkswaterstaat is acknowledged for providing historical bathymetric data of the Western Scheldt. This research is part of the project "Agenda voor de Toekomst," 14_094, which is funded by the Flemish-Dutch Scheldt Commission (VNSC). Historical bathymetric data of the Western Scheldt, Delft3D model input files, and model output data used to make the figures (including a metadata file, "Readme.docx") can be accessed online (https://doi.org/10.6084/m9.figshare.8783555.v1).

References

Ahlhorn, F., Meyerdirks, J., Heiber, W., & Saathoff, S. (2012, Secondary channels in European estuaries. Occurrence and Importance of Secondary Channels in European Estuaries - Literature Study in the framework of the Interreg project TIDE (Tech. Ref.). https://doi.org/10.13140/RG.2.1.1054.4166

Alebregtse, N. C., & de Swart, H. E. (2014). Effect of a secondary channel on the non-linear tidal dynamics in a semi-enclosed channel: A simple model. *Ocean Dynamics*, *64*(4), 573–585.

Deltares. (2016). User manual Delft3D-Flow: Simulation of multi-dimensional hydrodynamic flows and transport phenomena, including sediments (Tech. Rep.). Version 3.15, Delft, The Netherlands.

Egbert, G. D., & Erofeeva, S. Y. (2002). Efficient inverse modeling of barotropic ocean tides. *Journal of Atmospheric and Oceanic Technology*, *19*(2), 183–204.

Healy, M. & Hickey, K.R (2002). Historic land reclamation in the intertidal wetlands of the Shannon Estuary, Western Ireland. *Journal of Coastal Research*, *36*(SI), 365–373. https://doi.org/10.2112/1551-5036-36.sp1.365

Jeuken, M. (2000). On the morphological behaviour of tidal channels in the Westerschelde estuary (PhD thesis). Utrecht University, The Netherlands.

Kuijper, K., & Lescinski, J. (2012). Data analyses and hypotheses Western Scheldt (Tech. Rep.). Deltares, The Netherlands. Project number 1204405. 187p.

Li, C., Schuttelaars, H. M., Roos, P. C., Damveld, J. H., Gong, W., & Hulscher, S. J. M. H. (2016). Influence of retention basins on tidal dynamics in estuaries: Application to the Ems estuary. *Ocean and Coastal Management*, *134*, 216–225. https://doi.org/10.1016/j.ocecoaman.2016.10.010

Lucker, T., Busch, D., Knötzel, J., & Schirmer, M. (1995). Unterweserausbau, Entwicklung des Schiffsverkehrs und Auswirkungen auf das Flusssystem. *Die Weser Limnologie Aktuell*, *6*, 301–312.

Nnafie, A., Van Oyen, T., De Maerschalck, B., van der Vegt, M., & Wegen, M. V. D. (2018). Estuarine channel evolution in response to closure of secondary basins: An observational and morphodynamic modeling study of the Western Scheldt Estuary. *Journal of Geophysical Research: Earth Surface*, *123*, 167–186. https://doi.org/10.1002/2017JF004364

Pye, K., & Blott, S. J. (2014). The geomorphology of UK estuaries: The role of geological controls, antecedent conditions and human activities. *Estuarine, Coastal and Shelf Science*, *150*, 196–214. https://doi.org/10.1016/j.ecss.2014.05.014

Savenije, H. H. G., Toffolon, M., Haas, J., & Veling, E. J. M. (2008). Analytical description of tidal dynamics in convergent estuaries. *Journal of Geophysical Research*, *113*, C10025. https://doi.org/10.1029/2007JC004408

Sherwood, C. R., Jay, D. A., Harvey, R. B., Hamilton, P., & Simenstad, C. A. (1990). Historical changes in the Columbia River estuary. *Progress in Oceanography*, *25*(1-4), 299–352. https://doi.org/10.1016/0079-6611(90)90011-P

Van der Spek, A. (1997). Tidal asymmetry and long-term evolution of Holocene tidal basins in The Netherlands: Simulation of palaeo-tides in the Schelde estuary. *Marine Geology*, *141*(1), 71–90. https://doi.org/10.1016/S0025-3227(97)00064-9

Van der Wegen, M., & Roelvink, J. (2008). Long-term morphodynamic evolution of a tidal embayment using a two-dimensional, process-based model. *Journal of Geophysical Research*, *113*, C03016. https://doi.org/10.1029/2006JC003983

Van der Wegen, M. (2013). Numerical modeling of the impact of sea level rise on tidal basin morphodynamics. *Journal of Geophysical Research: Earth Surface*, *118*, 447–460. https://doi.org/10.1002/jgrf.20034

Van Maren, D. S., Oost, A. P., Wang, Z. B., & Vos, P. C. (2016). The effect of land reclamations and sediment extraction on the suspended sediment concentration in the Ems Estuary. *Marine Geology*, *376*, 147–157. https://doi.org/10.1016/j.margeo.2016.03.007

Winterwerp, J. C., Wang, Z. B., van Braeckel, A., van Holland, G., & Kösters, F. (2013). Man-induced regime shifts in small estuaries, II: A comparison of rivers. *Ocean Dynamics*, *63*(11-12), 1293–1306. https://doi.org/10.1007/s10236-013-0663-8

Woodruff, J. D., Martini, A. P., Elzidani, E. Z., Naughton, T. J., Kekacs, D. J., & MacDonald, D. G. (2013). Off-river waterbodies on tidal rivers: Human impact on rates of infilling and the accumulation of pollutants. *Geomorphology*, *184*, 38–50.

Yellen, B., Woodruff, J. D., Ralston, D. K., MacDonald, D. G., & Jones, D. S. (2017). Salt wedge dynamics lead to enhanced sediment trapping within side embayments in high-energy estuaries. *Journal of Geophysical Research: Oceans*, *122*, 2226–2242. https://doi.org/10.1002/2016JC012595